Quantitative real-time RT-PCR

$CD4^+$ T cells from human peripheral blood mononuclear cells (PBMCs) or murine lymphoid tissues were isolated by magnetic cell separation using anti-CD4 antibody (Miltenyi Biotec, Bergisch Gladbach, Germany). The total RNA was extracted using an RNeasy Mini Kit (Qiagen, Valencia, CA, USA). cDNA was obtained by reverse-transcription of mRNA with High-Capacity RNA-to-cDNA Master Mix (Applied Biosystems, Foster City, CA, USA). The miRNA fraction was prepared using an miRNA Isolation kit (Ambion, Austin, TX, USA), and 10 ng of total RNA were reverse-transcribed by a MicroRNA Reverse Transcription Kit (Applied Biosystems). Quantitative real-time reverse transcriptase polymerase chain reaction (qRT-PCR) analyses for GRAIL (human ID, Hs00226053; mouse ID, Mm00506597), FoxP3 (ID, Mm00475162), GITR (ID, Mm00437136), CTLA-4 (Cytotoxic T-Lymphocyte Antigen 4; ID, Mm00486849), β-actin, miR-290-5p (ID, 002590), and snoRNA135 (ID, 001234) were performed using ready-to-use assays in the ABI Prism 7900HT Sequence Detection System (Applied Biosystems). β-actin and snoRNA135 were used as the endogenous controls.

Immunoblot analysis

Human $CD4^+$ T cells from PBMC or murine $CD4^+$ T cells were lysed in radio-immunoprecipitation assay (RIPA) buffer. Protein samples were subjected to SDS-PAGE and transferred to a polyvinylidene difluoride membrane, as previously described [15]. The membrane was probed with rabbit anti-human GRAIL antibody (IMGENEX, San Diego, CA), rat anti-mouse GRAIL antibody (BD Biosciences, Franklin Lakes, NJ, USA) or rabbit anti-β-actin antibody (Cell Signaling Technology, Danvers, MA, USA). The blots were developed with horseradish peroxidase (HRP)-conjugated secondary antibodies and enhanced chemiluminescence (GE Healthcare).

Immunohistochemistry

Paraffin-embedded tissue sections were subjected to antigen retrieval by incubation in a pressurized heating chamber (Dako, Carpinteris, CA, USA). Tissue sections were reacted in combination with rat anti-mouse GRAIL antibody (BD Biosciences), rabbit anti-human GRAIL antibody (IMGENEX, San Diego, CA, USA), mouse anti-human CD4 antibody (Abcam, Cambridge, UK), or mouse anti-human FoxP3 antibody (Abcam) as first antibodies, followed by Alexa Flour 488®-labeled anti-rat or anti-rabbit IgG antibody (Molecular Probes, Eugene, OR, USA) or Texas Red-labeled anti-mouse IgG antibody (Abcam) as a secondary antibody. Nuclear staining was performed by DAPI (4′,6-diamidino-2-phenylindole). These stained samples were examined using fluorescence microscopy (Keyence, Osaka, Japan) or three-dimensional, structured illumination microscopy (Carl Zeiss, Oberkochen, Germany). In mice transferred with $GRAIL^{high}$ DO11.10 cells, the tissue sections were stained with anti-mouse GFP antibody (Clontech), and color was developed by 3′-diaminobenzidine using a VECTASTAIN ABC kit (Vector Laboratories, Burlingame, CA, USA).

miRNA microarray analysis

For the miRNA microarray analysis, 0.5 μg of total RNA from $CD4^+$ T cells of the SP or LP were labeled using a miRCURY LNA™ microRNA Array Power Labeling kit (Exiqon, Vedbaek, Denmark) according to the manufacturer's instructions. Each sample of RNA labeled with Hy5 was hybridized with a highly sensitive DNA chip, *3D-Gene*™ (Toray Industries, Tokyo, Japan) at 37 °C for 16 h. Hybridization signals derived from Hy5 were scanned using a 3D-Gene Scanner (Toray). The scanned image was analyzed and scaled by global normalization [22]. All microarray experiments were performed in compliance with MIAME (Minimum Information About a Microarray Experiment) guidelines [23].

miRNA target predictions

miRgator (http://mirgator.kobic.re.kr:8080/MEXWebApp/), miRGen (http://www.diana.pcbi.upenn.edu/cgi-bin/miRGen/v3/Targets.cgi), and MicroCosmTargets (http://www.ebi.ac.uk/enright-srv/microcosm/htdocs/targets/v5/) were used to predict miRNAs that potentially combine with the 3′-untranslated region (3′UTR) of GRAIL mRNA.

Transfection

DO11.10 cells (a murine T cell line, purchased from European Collection of Cell Cultures, Salisbury, UK) were transfected with anti-miR-290-5p inhibitor (50 nM, Ambion) by electroporation (250 V, 950 μF). Anti-miRNA Inhibitors Negative Control #1 (Ambion) was used as endogenous control. Seventy-two hours after the transfection of anti-miR-290-5p inhibitor or negative control #1, cells were collected, and cellular lysates were subjected to western blot using an anti-GRAIL antibody. The GRAIL fragment was inserted into a pAcGFP vector (Clontech, Palo Alto, CA, USA), and the pAcGFP-GRAIL vector or empty vector was transfected into DO11.10 cells by X-tremeGENE HP (Roche, Basel, Switzerland) according to the manufacturer's instructions. $EGFP^+$ DO11.10 cells ($2–5 \times 10^4$ cells/body) sorted by flow cytometry (FACSAria™ II) were intravenously injected into

C57BL/6J mice 2 days after the 2 % DSS administration. The body weight, and the length and histology of the colon were evaluated on day 9.

Luciferase assay

Synthesized oligonucleotides of GRAIL-3′UTR construct, which contained putative miR-290-5p binding sites, were inserted downstream of Luciferase in a pMIR-REPORT Luciferase vector (Ambion). PGL4 *Renilla* Luciferase vector (Promega, Madison, WI, USA) was used to compensate for the transfection efficacy. These constructs and pre-miR 290 precursors (40 nM) or pre-miR^{TM} miRNA negative controls #1 (Ambion) were co-transfected into NIH-3T3 (murine fibroblast cell line) using Lipofectamine 2000 (Invitrogen). Firefly luciferase activity was measured 48 h after transfection using a Dual-Glo^{TM} Luciferase Assay System (Promega). The firefly luciferase activity was evaluated after the compensation by *Renilla* luciferase activity.

Histological analysis

Histological scores for DSS colitis were determined, as previously described, as the sum of the following scores [24]: changes in the epithelium (0, normal; 1, focal loss of goblet cells; 2, diffuse loss of goblet cells; 3, focal loss of crypts; 4, diffuse loss of crypts) and for cell infiltration (0, no increase; 1, around bases of the crypts; 2, diffuse infiltration along the layer of muscularis mucosae; 3, complete infiltration of the mucosal layer; 4, infiltration of both mucosal and submucosal layers).

Cytokine ELISA

DO11.10 cells were transfected with pAcGFP-GRAIL or an empty vector as control, and AcGFP$^+$ T cells were sorted using flow cytometry 48 h after the transfection. Culture supernatants of the cells were collected after activation with plate-coated, anti-CD3 antibody (5 μg/ml) and soluble, anti-CD28 antibody (5 μg/ml), and were analyzed by IL-10, TGF-β, and IL-2 ELISA kit according to manufacturer's instructions (eBioscience, San Diego, CA, USA).

Statistical methods

Student's *t* test, the Wilcoxon signed-rank test and the Tukey HSD test were used for statistical analysis. The body weight of mice injected with DO11.10 was evaluated by a two-factor, repeated ANOVA. $P < 0.05$ was considered statically significant and data were presented as the mean + SEM.

Ethical considerations

The Institutional Review Board of Osaka University Hospital approved the human study protocol, and written informed consent was obtained from each participant. The Institutional Animal Committee on Animal Research approved the mouse protocol.

Results

Expression of GRAIL mRNA and protein in CD4$^+$ T cells in the peripheral blood of the patients with CD

We examined the expression of GRAIL in the peripheral blood of 37 patients with CD and 22 healthy volunteers (HV). The characteristics of the subjects are listed in Table 1. The GRAIL mRNA levels in the CD4$^+$ T cells were significantly lower in the peripheral blood of the patients with active CD than in the HV (Fig. 1a). In addition, the GRAIL mRNA levels were significantly lower even in the CD patients in remission than in the HV (Fig. 1a). Consistent with the lower GRAIL mRNA expression in CD, the protein levels of GRAIL were lower in the peripheral blood CD4$^+$ T cells of the CD patients than in those of the HV (Fig. 1b). These results were different from our previous results of UC patients, where GRAIL mRNA in the remissive UC patients was higher than in healthy volunteers and the expressions of active UC patients and healthy volunteers were not statistically different [15]. We also investigated the expression of GRAIL in the peripheral blood of *Il-10*$^{-/-}$ mice. *Il-10*$^{-/-}$ mice develop spontaneous chronic intestinal inflammation at approximately 4 weeks of age, while *Il-10*$^{+/-}$ mice lack this inflammation. The levels of GRAIL mRNA in the peripheral blood CD4$^+$ T cells were lower in *Il-10*$^{-/-}$ mice

Table 1 Clinical characteristics of the patients

	CD (active)	CD (remission)	HV
Gender (M/F)	13/4	14/6	16/6
Disease type (ileal/colonic/ileo-colonic)	9/2/6	8/7/5	–
Age[a]	38.2 (±11.7)	40.0 (±13.9)	35.6 (±7.7)
CDAI[a]	251.1 (±69.3)**	85.2 (±30.9)	–
CRP (mg/l)[a]	13.6 (±20.3)***	4.1 (±6.6)	–

CD Crohn's disease, *HV* healthy volunteers, *CDAI* Crohn's disease activity index, *CRP* C-reactive protein

[a] Mean (±SEM)

** $P < 0.05$

*** $P < 0.01$, compared with CD in remission

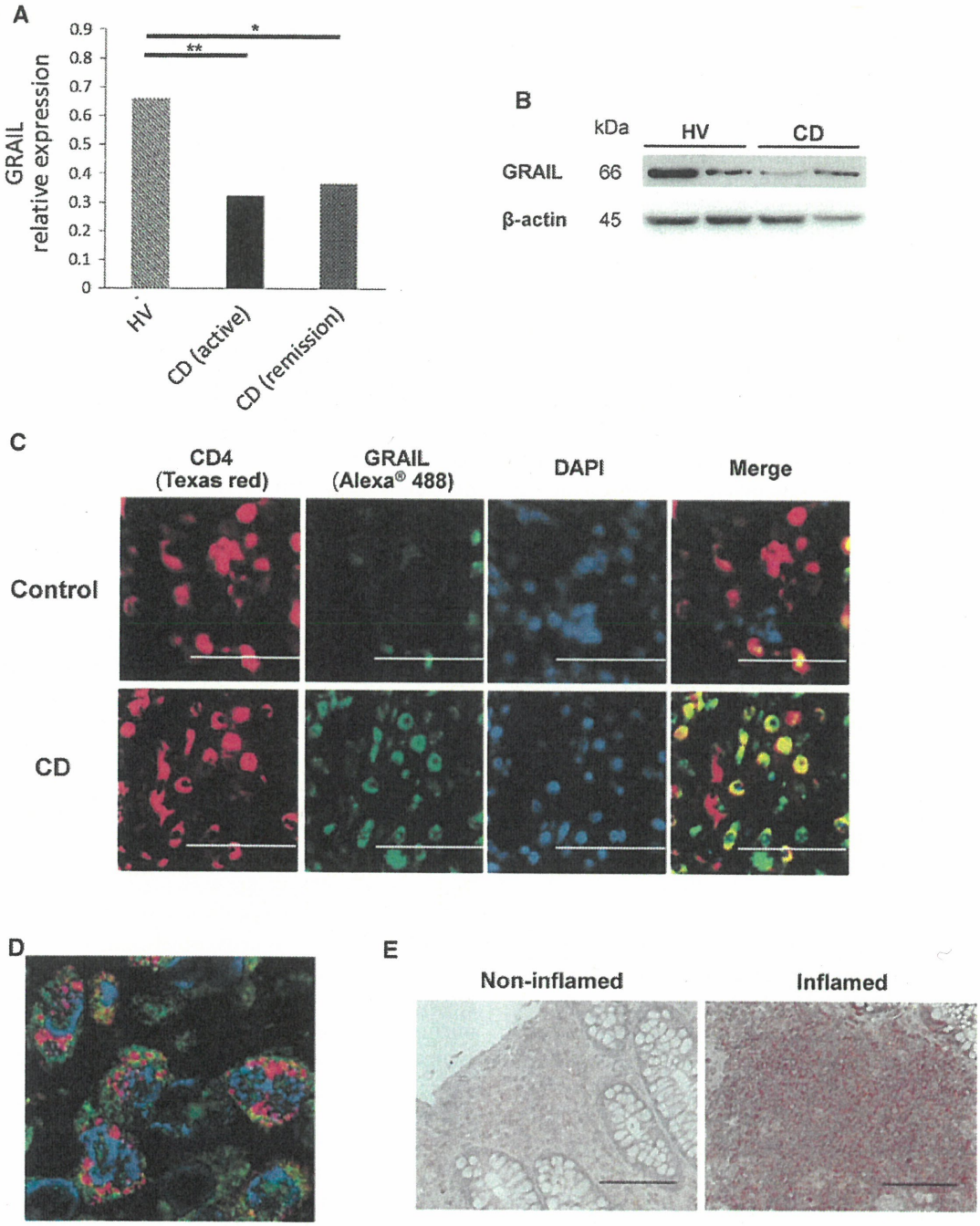

Fig. 1 Expression of GRAIL is lower in the peripheral $CD4^+$ T cells, but higher in the LP of Crohn's disease. **a** Levels of GRAIL mRNA in the peripheral blood $CD4^+$ T cells isolated from 22 healthy volunteers (HV), 17 active patients with CD, and 20 patients with CD in remission were analyzed by qRT-PCR. GRAIL mRNA was significantly lower in the $CD4^+$ T cells of active and remissive CD patients than in HV. Data are shown as the mean + SEM. $*P < 0.05$; $**P < 0.01$. **b** GRAIL protein expressions of the peripheral blood $CD4^+$ T cells isolated from HV and the patients of CD were analyzed by western blot. Representative blots from HV and active CD patients are shown. **c** Immunohistochemical staining of non-inflamed colonic mucosa of colon cancer patients (control) and inflamed mucosa of CD patients. Colonic tissues were stained with Texas red-labeled anti-CD4 antibody (*red*), Alexa®488-labeled anti-GRAIL antibody (*green*) and DAPI (*blue*). *Scale bar* 50 μm. **d** The LP mononuclear cells of patients with CD were stained with CD4-Texas red (*red*), GRAIL-Alexa®488 (*green*) and DAPI (*blue*), and subjected to three-dimensional, structured illumination microscopy. **e** Specimens from non-inflamed and inflamed colonic mucosa were stained by anti-GRAIL antibody and color was developed by 3, 3′-diaminobenzidine. GRAIL-stained cells (*brown*) were massively observed in the LP of inflamed lesion. *Scale bar* 100 μm (color figure online)

than in *Il-10*$^{+/-}$ mice, consistent with the reduced protein expression of GRAIL in *Il-10*$^{-/-}$ mice (Supplementary Fig. 1A, B).

Expressions of GRAIL mRNA and protein in CD4$^+$ T cells in the intestinal lamina propria of the patients with CD

Next, we examined GRAIL protein expression in the intestinal LP of CD patients and control subjects by immunohistochemistry. The GRAIL-positive cells were highly observed in the intestinal CD4$^+$ T cells of the patients with CD in contrast to the infrequent GRAIL-positive cells in control subjects (Fig. 1c, Supplementary Fig. 2A). When we investigated the GRAIL protein expression by three-dimensional, structured illumination microscopy, GRAIL was ubiquitously expressed in the cytoplasm, suggestive of endosomes, of CD4$^+$ T cells in the intestinal LP of the patients with CD (Fig. 1d). In addition, the expression of GRAIL was massively observed in severely inflamed lesions with erosions and ulcers, rather than in non-inflamed lesions (Fig. 1e). In contrast, GRAIL mRNA expressions were not significantly different between the colonic tissue samples of CD and the control subjects (Supplementary Fig. 2B). Thus, we observed discrepant patterns of GRAIL expression between the peripheral blood and the intestinal LP in patients with CD.

Discrepant GRAIL mRNA and protein expressions in the colonic CD4$^+$ T cells of dextran sodium sulfate-induced colitis

We next investigated the expression of GRAIL in the lymphoid organs of DSS-induced, acute murine colitis. The level of GRAIL mRNA was significantly lower in the LP CD4$^+$ T cells of mice with DSS colitis than in those of mice untreated with DSS (Fig. 2a). In contrast, the GRAIL protein level in the LP CD4$^+$ T cells of colitic mice was significantly higher than that of untreated mice (Fig. 2b, c). The level of GRAIL mRNA in CD4$^+$ T cells was significantly higher in the LP than in the SP or MLN of untreated mice (Fig. 2a). In contrast, the GRAIL protein level was lower in the CD4$^+$ T cells in the LP than in those in the SP and MLN of untreated mice (Fig. 2b, c).

Discrepant expressions between the GRAIL mRNA and protein in the colonic CD4$^+$ T cells of *Il-10*$^{-/-}$ mice

When the GRAIL mRNA was compared between *Il-10*$^{-/-}$ and *Il-10*$^{+/-}$ mice, the level of GRAIL mRNA was significantly lower in the LP CD4$^+$ T cells of colitic *Il-10*$^{-/-}$ mice than those of non-colitic *Il-10*$^{+/-}$ mice (Fig. 2d). In contrast, the level of GRAIL protein in the LP was significantly higher in *Il-10*$^{-/-}$ mice than in *Il-10*$^{+/-}$ mice (Fig. 2e, f). Thus, the GRAIL mRNA and protein expression patterns of *Il-10*$^{-/-}$ mice were similar to those of mice with DSS colitis in terms of the discrepancy of GRAIL mRNA and protein levels in the LP between colitic and non-colitic mice. In addition, there was a discrepancy of GRAIL mRNA and protein between the SP and LP in the non-colitic mice, showing high mRNA levels but low protein levels of GRAIL in the LP compared to the SP. It has been shown that the specific deubiquitinating enzyme (DUB), Otub-1, induces degradation of GRAIL [10, 25]. We speculated that the suppression of Otub-1 might upregulate GRAIL expression via the abrogation of deubiquitination of GRAIL in the LP of colitic mice. The levels of Otub-1 mRNA, however, were not significantly different among CD4$^+$ T cells in the SP, MLN, and LP of *Il-10*$^{+/-}$ and *Il-10*$^{-/-}$ mice (Supplementary Fig. 3A). In addition, the levels of ubiquitination of the GRAIL protein in the CD4$^+$ T cells of SP and LP were not different in both *Il-10*$^{+/-}$ and *Il-10*$^{-/-}$ mice (Supplementary Fig. 3B). These results indicated that Otub-1 does not play a major role for the regulation of GRAIL in murine colitis.

miR-290-5p as a novel miRNA related to the regulation of GRAIL

miRNAs, a novel class of non-coding small RNAs, repress gene expression by binding to the 3′UTR of target messenger RNAs, thereby suppressing protein expression [26]. We screened miRNAs that were highly expressed in the LP relative to the SP by miRNA microarray, using samples of SP and LP CD4$^+$ T cells isolated from *Il-10*$^{+/-}$ mice, because there was a discrepancy between the mRNA and protein levels in these two lymphoid organs. The miRNA microarray revealed upregulation of 58 miRNAs in the LP, compared with SP (GEO accession number; GSE40891). Among these upregulated miRNAs, computational predictions revealed that miR-26b, miR-295, miR-330, miR-290-5p, and miR-290-3p had a potential to bind to the 3′UTR of GRAIL and miR-290-5p was expressed more than two-fold higher in the LP than in the SP (Table 2). The seed lesion of miR-290-5p completely coincided with the putative GRAIL-3′UTR (Fig. 3A). We next analyzed the expression of miR-290-5p in the CD4$^+$ T cells of the systemic and mucosal lymphoid tissues of *Il-10*$^{+/-}$ and *Il-10*$^{-/-}$ mice by qRT-PCR. miR-290-5p was confirmed to be expressed significantly higher in the LP than in the SP of *Il-10*$^{+/-}$ mice (Fig. 3b). In addition, the expression of miR-290-5p in the CD4$^+$ T cells of the LP was significantly higher in *Il-10*$^{+/-}$ mice than in *Il-10*$^{-/-}$ mice. The miR-290-5p levels in the SP and MLN were not significantly different between *Il-10*$^{+/-}$ and *Il-10*$^{-/-}$ mice (Fig. 3b).

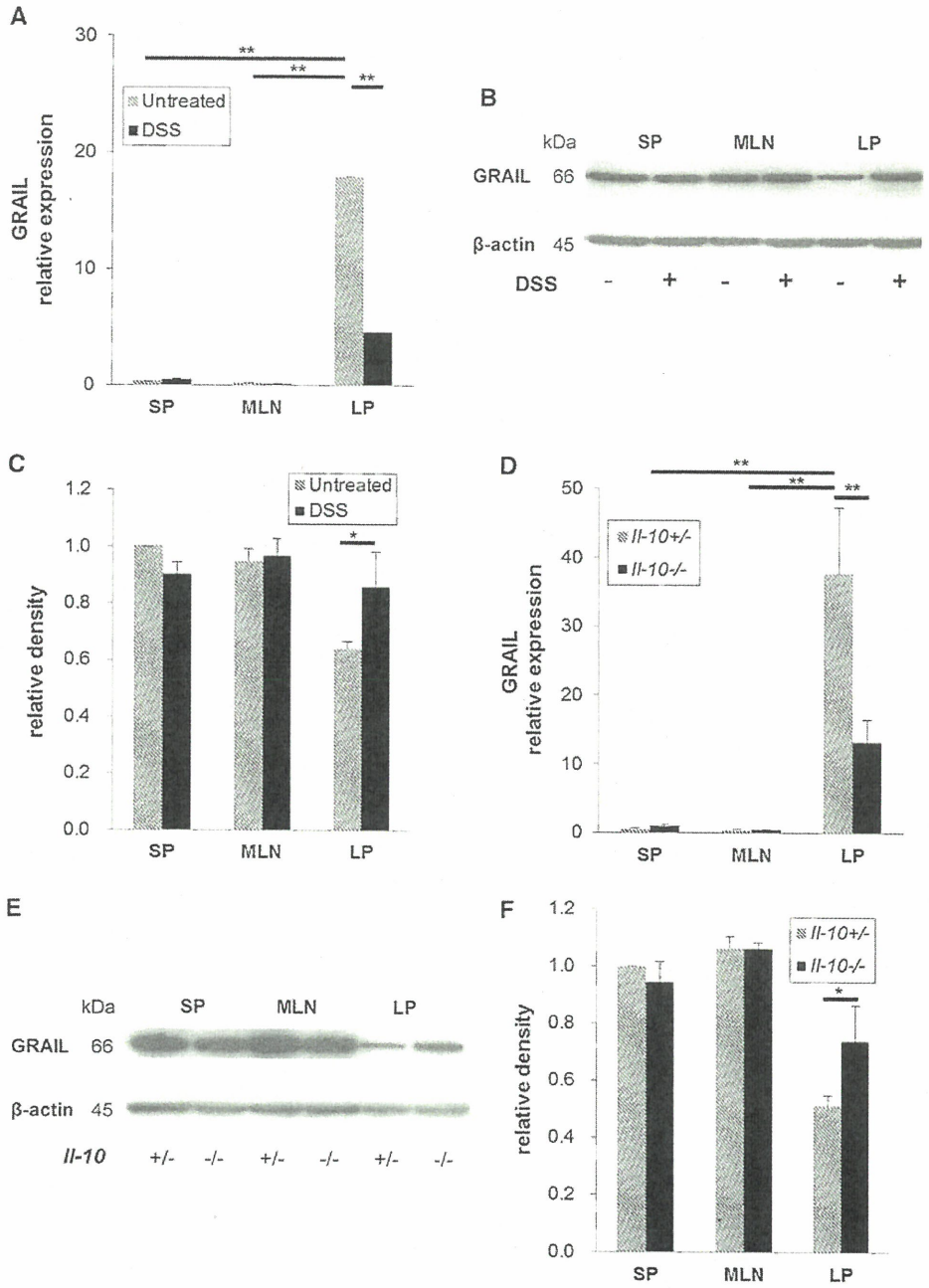

Fig. 2 Discrepancy between GRAIL mRNA and protein expressions in the lamina propria of murine colitis. **a** The levels of GRAIL mRNA were evaluated in mice induced with DSS colitis. GRAIL mRNA was significantly higher in the $CD4^+$ T cells of the LP than in those of the SP and MLN in untreated mice. GRAIL mRNA was significantly lower in the LP of DSS-treated mice (*solid bar*) than mice untreated with DSS (*shaded bar*; $n = 8$ in each group; $^{**}P < 0.01$). **b** The GRAIL protein levels in the $CD4^+$ T cells isolated from lymphoid tissues were analyzed by western blot in mice treated with DSS (+) or without DSS (−). Representative pictures of three independent experiments are shown. **c** Band intensities were quantified by densitometry. The data were expressed as mean + SEM from three separate experiments. $^*P < 0.05$. **d** The mRNA expressions of GRAIL in $CD4^+$ T cells of the SP, MLN, and LP of *Il-10*$^{+/-}$ and *Il-10*$^{-/-}$ mice (age 10–12 weeks) were determined by qRT-PCR ($n = 8$). The levels of GRAIL mRNA in the LP were significantly higher than in other lymphoid tissues in *Il-10*$^{+/-}$ mice. GRAIL mRNA of the LP was higher in *Il-10*$^{+/-}$ mice (*shaded bar*) than in *Il-10*$^{-/-}$ mice (*solid bar*; $^{**}P < 0.01$). E. The levels of GRAIL protein in $CD4^+$ T cells of the SP, MLN, and LP of *Il-10*$^{+/-}$ and *Il-10*$^{-/-}$ mice were analyzed by western blot. Representative pictures from three independent experiments are shown. **f** Band intensities were quantified by densitometry. The data were expressed as mean + SEM from three separate experiments. $^*P < 0.05$